Available online at www.sciencedirect.com
SCIENCE DIRECT®
Journal of Organometallic Chemistry 691 (2006) 2162–2170
Journal of Organometallic Chemistry
www.elsevier.com/locate/jorganchem

A new type of chiral porphyrin: Organopalladium porphyrins with chiral chelating diphosphine ligands

Margaret J. Hodgson [a], Victor V. Borovkov [b], Yoshihisa Inoue [b], Dennis P. Arnold [a,*]

[a] *Synthesis and Molecular Recognition Program, School of Physical and Chemical Sciences, Queensland University of Technology, G.P.O. Box 2434, Brisbane 4001, Australia*
[b] *Entropy Control Project, ICORP, JST, 4-6-3 Kamishinden, Toyonaka-shi, Osaka 560-0085, Japan*

Received 15 August 2005; received in revised form 4 October 2005; accepted 5 October 2005
Available online 11 November 2005

Abstract

Peripherally palladated Ni(II) porphyrins have been prepared using enantiopure chiral chelating diphosphines as supporting ligands on the attached Pd(II) fragment. Both enantiomers of the following complexes have been obtained in good yields, using oxidative addition of the bromoporphyrin starting material 5-bromo-10,20-diphenylporphyrinatonickel(II) (NiDPPBr (**1**)) to the [Pd^0L] complex generated in situ from Pd_2dba_3 and the chiral ligand L: [PdBr(NiDPP)(CHIRAPHOS)] (**2a**,**b**) [CHIRAPHOS = 2,3-bis(diphenylphosphino)butane], [PdBr(NiDPP)(Tol-BINAP)] (**3a**,**b**) [Tol-BINAP = 2,2′-bis(di-*p*-tolylphosphino)-1,1′-binaphthyl] and [PdBr(NiDPP)-(diphos)] [diphos = 1,2-bis(methylphenylphosphino)benzene] (**4a**,**b**). The induced asymmetry in the porphyrin was readily detected by ^{1}H NMR and CD spectroscopy. The porphyrin chiroptical properties are strongly dependent upon the structure of the chiral ligand, such that a monosignate CD signal, and symmetric and asymmetric exciton couplets were observed for **4a**, **2b**, and **3a**,**b**, respectively.

Keywords: Organopalladium porphyrin; Chiral porphyrin; Chiral diphosphine; Circular dichroism

1. Introduction

Porphyrins have fascinated scientists for many years due to their unique roles in biology. In recent years, a vast array of novel porphyrinoid structures has been prepared and investigated for both fundamental scientific and applied technological reasons [1]. The introduction of chirality into porphyrin structures may lead to major applications in chiral recognition [2–8] and enantioselective catalysis [9–11], using the coordinating ability and catalytic propensity of the metal ion coordinated centrally within the chiral environment. Most of these chiral porphyrins have been prepared using chiral substituent groups attached to peripheral *meso* and/or β carbons (Scheme 1) of the ring, particularly using, for ease of synthesis, chiral attachments to *meso*-aryl groups in 5,10,15,20-tetraarylporphyrins. In some cases, these groups are designed to offer additional supramolecular coordination properties to increase the number of contact points between the porphyrin-based receptor and the substrate [2]. In addition, intrinsically achiral bis(porphyrins) have been used as chiral reporter groups due to the induction of chirality in the porphyrin chromophore by chiral hosts. These supramolecular systems have been effectively applied for the determination of the absolute configuration of various chiral compounds [12,13], selective sensing of saccharides, cysteine polyion, and mandelic acid [14–16], and chiral memory elements [17,18].

Chiral chelating diphosphine ligands have assumed importance in enantioselective reactions catalyzed by transition metal complexes, such as those involving palladium [19]. We have tried to combine porphyrin-based chiral receptors and potential transition metal catalytic sites, taking advantage of the fact that enantiopure chiral diphosphine ligands are now commercially available.

* Corresponding author.
E-mail address: d.arnold@qut.edu.au (D.P. Arnold).

0022-328X/$ - see front matter © 2005 Elsevier B.V. All rights reserved.
doi:10.1016/j.jorganchem.2005.10.014

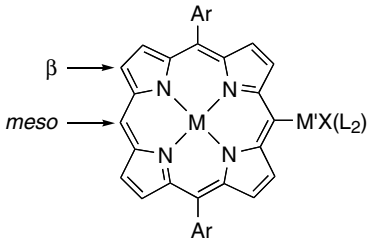

Scheme 1. The general structure of peripherally metallated porphyrins (M′ = Pd, Pt).

"Organometallic porphyrins" of various structural types have been known for many years [20], but since 1998, we have been studying a previously neglected class, namely peripherally palladated and platinated porphyrins, of the type represented by the general structure shown in Scheme 1, in which the metallo substituent is attached at one (or two) *meso* positions. We have prepared numerous examples in which we varied the lateral aryl substituents (Ar = phenyl, *p*-tolyl, 3,5-di-*tert*-butylphenyl) on the 10,20 porphyrin carbons, the centrally coordinated metal ion (M = 2H, MnCl, Co, Ni, Zn, InCl), the neutral ligands (L_2 = monodentate aryl or alkyl phosphines, chelating diphosphine, chelating diamine), and the external ligand (X = Br, Cl, NO_3, CF_3SO_3, pyridines, pyridyl porphyrins). Syntheses, spectra, crystal structures, electrochemistry and uses as synthetic intermediates have been described [21–28]. For chelating diphosphines, only the Pd(II) complexes have been prepared [21,22,27], while for monodentate phosphines and chelating diamines, both Pd(II) and Pt(II) systems are known [23–25]. Palladium catalysis has recently been used to prepare chiral 5,15-disubstituted derivatives of diarylporphyrins, but the ligands on the palladium were not themselves chiral [29]. It is expected that the combination of a chiral porphyrin receptor with a catalytically active transition metal site near the periphery may lead to new unique enantioselective processes and functions. We now report our initial studies of the incorporation of chiral diphosphine ligands into organopalladium(II) porphyrins. This work has been carried out, as proof of concept, with the Ni(II) complex of 5,15-diphenylporphyrin (NiDPP) as the porphyrin core. Measurement of the circular dichroism (CD) spectra has revealed chiral induction in the porphyrin unit by the bulky chiral ligands. This paper reports the synthesis and characterization, particularly by NMR and CD spectroscopy, of three pairs of enantiomeric complexes, using three different classes of chiral diphosphine (Scheme 2).

2. Results and discussion

2.1. Synthesis

The suite of new chiral derivatives **2**–**4** was prepared according to the methods we have used previously for achiral diphosphine ligands, namely oxidative addition of *meso*-bromoporphyrin (**1**) to Pd(0) diphosphine precursors [21,22,27]. The latter were prepared in situ by reaction of the diphosphine ligand with Pd_2dba_3 (dba = dibenzylideneacetone) in hot toluene under argon atmosphere (Scheme 2). The enantiomeric pairs of three types of chiral diphosphine (Scheme 2) were employed, in order to explore the influences of the different types on the NMR and CD spectra of the porphyrins. The first, represented by CHIRAPHOS [2,3-bis(diphenylphosphino)butane], is chiral by virtue of the two chiral carbons in the backbone. The second is Tol-BINAP [2,2′-bis(di-*p*-tolylphosphino)-1,1′-binaphthyl], which is chiral due to atropisomerism about the binaphthyl bond. The final one [abbreviated here as "diphos", 1,2-bis(methylphenylphosphino)benzene] is

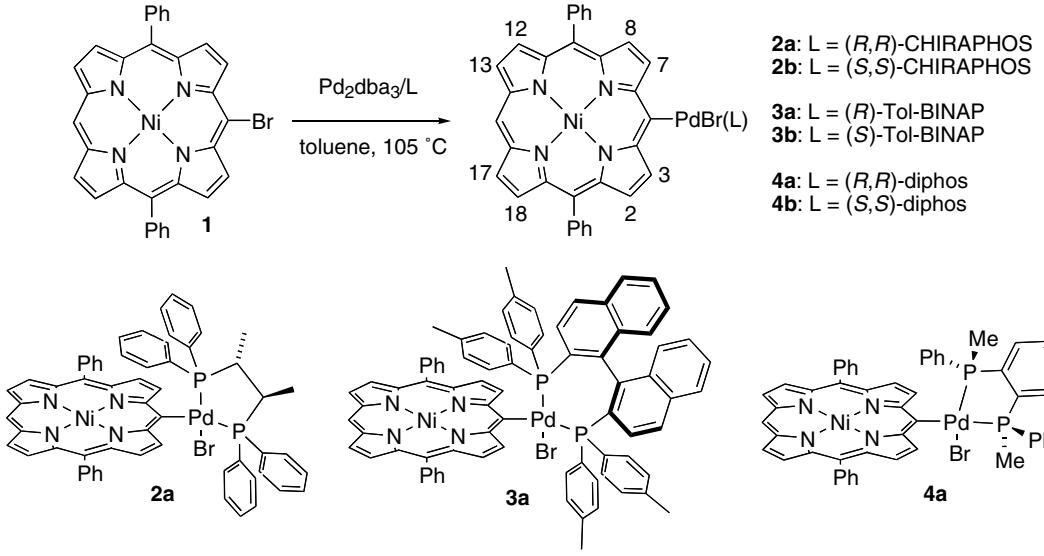

Scheme 2. Synthetic method, list of compounds, structures of the chiral complexes, [represented by the respective (*R*)- or (*R*,*R*)-isomers] and the numbering of the porphyrin ring carbons.

chiral at both phosphorus atoms [30]. The reactivity of the PdL fragments clearly decreases in the order diphos > CHIRAPHOS > Tol-BINAP, as judged by the rate of completion of the reaction. This is in the same order as the expected decrease in electron density on the phosphorus atoms attached to the Pd(0), although it is also the order of increasing bulkiness of the ligand. On the other hand, the ligand that appeared to generate the most reactive Pd(0) nucleophile in our previous studies, 1,1′-bis(diphenylphosphino)ferrocene (dppf), is also rather bulky [22], so a decision on the relative influences of these factors is not yet clear.

The reactions were followed by thin layer chromatography (TLC) until the starting bromoporphyrin **1** was consumed. The Pd porphyrins decompose on the TLC plates, forming NiDPP, so the formation of the Pd species cannot be followed *directly* by TLC [27]. The diphos complexes **4a**,**b** precipitated from hot toluene within 15 min, while the other two ligands yielded complexes that were soluble in toluene. The diphos complexes are rather unstable in chlorinated solvents, decomposing to NiDPP and (presumably) Pd(diphos) dihalide complexes. This decomposition prevented a thorough study of the complexes of this ligand, as their low solubility prevented examination in other solvents. The Tol-BINAP complexes **3a**,**b** were the most stable in solution, and could be recrystallised from CH_2Cl_2/hexane. The CHIRAPHOS complexes **2a**,**b** were isolated by the precipitation with hexane from the concentrated reaction mixture in toluene. The products were characterised by the ^1H and $^{31}P\{^1H\}$ NMR, FAB-mass, and UV–Vis and CD spectra, and in the case of {PdBr(NiDPP)[(*S*,*S*)-(CHIRAPHOS)]} (**2b**), by CHN analysis.

2.2. NMR spectra

As is typical for chelating bisphosphine palladium(II) complexes, the $^{31}P\{^1H\}$ NMR spectra exhibit a pair of doublets due to P–P coupling between the non-equivalent ^{31}P nuclei. The ^2J(P–P) values decrease in the order CHIRAPHOS (38.5) > Tol-BINAP (37.4) > diphos (23.3 Hz), while the chemical shifts lie in the order CHIRAPHOS (58.9, 41.8), Tol-BINAP (44.2, 36.3), diphos (25.0, 11.9 ppm). The ^1H NMR spectra are, as expected, rather complex, and deserve more discussion, as these are the first chiral organopalladium complexes to be isolated for porphyrins.

The downfield region of the spectrum of the (*R*,*R*)-CHIRAPHOS complex **2a** (Fig. 1) gives a clear indication of the asymmetry of the complex, by the presence of eight separate one-proton doublets for the eight porphyrin β protons, in addition to a singlet for the unique 15-*meso* proton (Schemes 1 and 2 show the numbering and nomenclature of the porphyrin carbons). One of the phenyl groups of the diphosphine ligand appears at rather high field, in the 5–5.5 ppm range, because of its average position in the porphyrin shielding zone. Two-dimensional COSY and ROESY spectra were collected to try to assign the protons completely, but while all through-bond correlations were obtained, some dipolar couplings could not be identified, including those for the porphyrin 10,20-phenyl groups with their adjacent β protons. Therefore, the latter could not be assigned individually, but only pair-wise. The methyl groups on the five-membered chelate ring appear as doublets of doublets due to the coupling with their partner CH and the adjacent ^{31}P. These couplings were defined by *J*-resolved spectra. The CH protons appeared as complex multiplets. Dipolar couplings from these backbone protons to *ortho*-protons of the P-phenyl groups were observed in some, but not all, cases, leaving some ambiguities in the assignments of the phenyl groups. A minor impurity with similar chemical shifts was also present; this is the corresponding chloro complex, formed by exchange of the bromide for chloride in the chlorinated solvent. We have observed this behaviour for other organopalladium and -platinum porphyrins [21–23], and confirmed the origin of the impurities. Upon standing in the solvent during the acquisitions of the 2D spectra, the characteristic peaks of unsubstituted NiDPP slowly increased in intensity, but the proportion decomposed reached only ca. 5% after 24 h.

The complexes **3a**,**b** containing the Tol-BINAP ligand gave very complex ^1H NMR spectra, as expected, due to

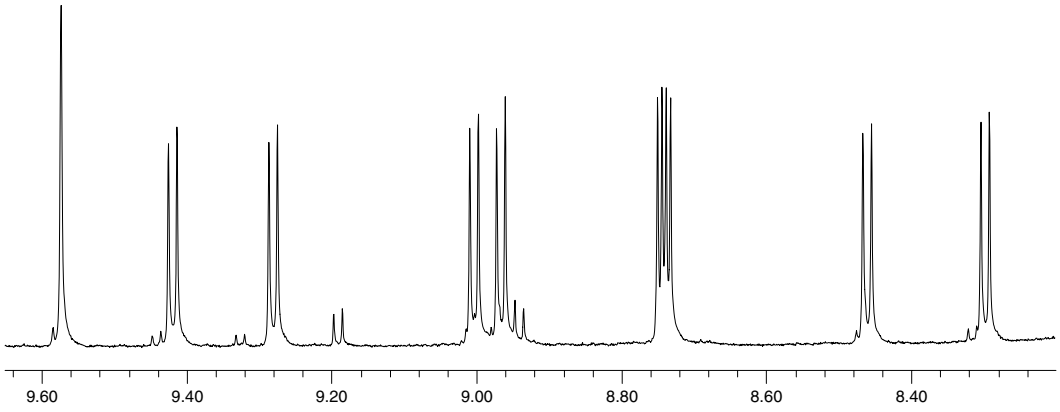

Fig. 1. Porphyrin proton region of the 400 MHz ^1H NMR spectrum of {PdBr(NiDPP)[(*R*,*R*)-CHIRAPHOS]} (**2a**) in $CDCl_3$. The minor doublets near 9.20 and 8.95 ppm are due to NiDPP, and the other small signals are due to the chloro analogue of **2a**.

the asymmetry and the large number of non-equivalent aromatic protons. We will discuss this spectrum in detail, because some interesting consequences of the ligand structure are apparent. One of the tolyl CH_3 singlets appears at quite high field, 0.31 ppm. The methyl groups for the other three tolyl groups resonate at 1.70, 2.06 and 2.53 ppm. This large spread is due to the magnetic anisotropy of the porphyrin ring, and perhaps also the binaphthyl rings. For comparison, note that the methyl groups of the free ligand resonate as two singlets near 2.2 ppm. The remaining signals for **3** span the range 4.6–10 ppm, as shown in Fig. 2 (upper). Individual assignments of the porphyrin ring protons are again not possible, although the pairs on each pyrrole ring were readily identified by COSY and ROESY spectra. The 2,3/7,8 pairs (see Scheme 2 for ring numbering) resonate as doublets at 10.02, 8.76/9.81, 8.59 ppm. The 13- and 17-Hs were identified from the dipolar coupling to the *meso*-H as doublets at 8.98 and 8.96 ppm, and their scalar coupled partners appear at 8.80 and 8.71 ppm, respectively. The fact that two of these protons resonate so far downfield (i.e. 10.02, 9.81 ppm; compare the CHIRAPHOS analogues at 9.41, 9.27), is rather striking for a Ni(II) porphyrin. It appears, therefore, that these protons come under the deshielding influence of one or more of the aryl rings of the ligand. Severe out-of-plane distortion of the porphyrin ring due to the presence of the bulky substituent would normally induce upfield shifts due to decreased aromaticity.

By examining the integrals, it became apparent that some protons seemed to be "missing". This matter was resolved by examination of spectra at reduced temperatures. But we will first describe the assignments that can be achieved from the room temperature spectrum. It may be helpful to examine Fig. 2 in conjunction with the structures in Fig. 3, which are different views of the minimized structure of the (*R*)-Tol-BINAP complex calculated at PM3(tm) semi-empirical level using the SPARTAN 02 program. The signals at 4.67 and 4.84, representing 4 Hs, are due to the *m*- and *o*-Hs of one tolyl ring. In an expanded view, these show the expected P–H couplings as well as the *o*-coupling between neighbouring protons on an aryl ring. The ROESY correlation of the 4.67 ppm signal with the highest field methyl signal (0.31 ppm) suggests this is the ring that lies over the plane of the porphyrin (Fig. 3), as this methyl group would surely experience the greatest upfield shift due to the magnetic anisotropy of the porphyrin macrocycle. These signals will be mentioned again below, when the effects of lowering the temperature are described. From the *o*-protons, there is a dipolar coupling to a signal (another pseudo-triplet, actually a doublet of doublets due to P–H and H–H coupling) at 8.32 ppm. This signal integrates for only one H, so it would appear to be the *o*-H on one side of a neighbouring tolyl ring. This proton also exhibits the only dipolar coupling that was observed from a non-porphyrin proton to one of the β protons, the one at 8.91 ppm. However, from this point, the correlation path was lost, and a single assignment eluded our efforts. The BINAP protons appear as several triplets and doublets across the aromatic region, overlapping with some of the porphyrin 10,20-phenyl signals.

Returning to the problem of the "missing" tolyl group, it can be seen in the room temperature spectrum in Fig. 2, that there is a very broad feature in the region 5–6.5 ppm (shown by the horizontal bracket in Fig. 2, upper). Upon

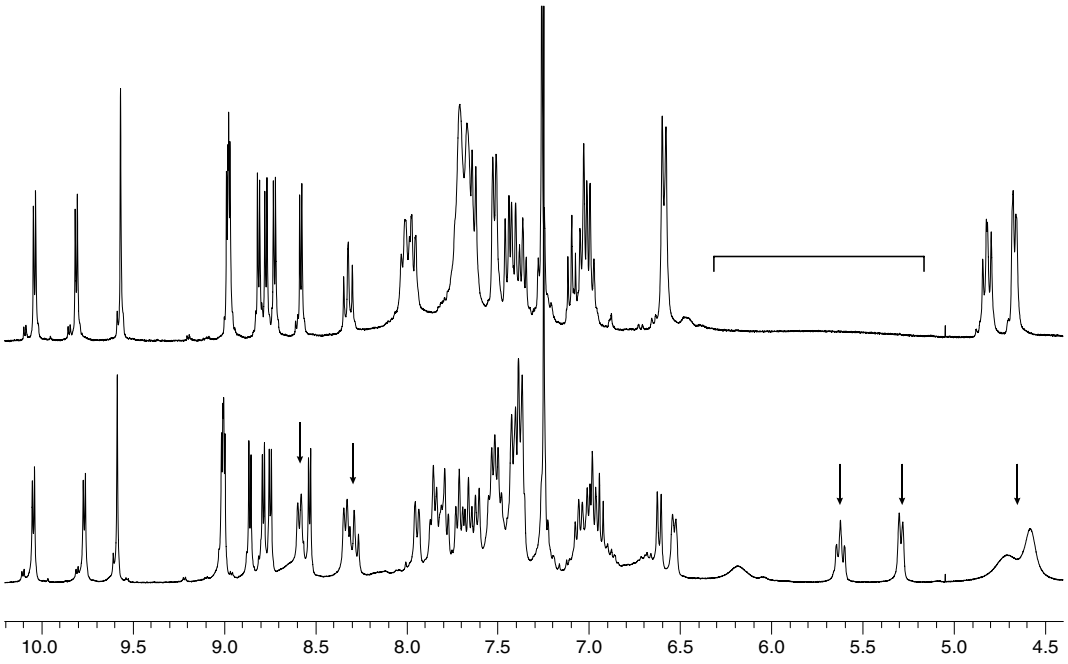

Fig. 2. Porphyrin and phosphine aryl region of the 400 MHz ^{1}H NMR spectrum of {PdBr(NiDPP)[(*R*)-Tol-BINAP]} (**3a**) in $CDCl_3$; upper: 288 K; lower: 218 K. In the text, particular mention is made of the region shown by the horizontal bracket (upper) and the signals marked by the arrows (lower).

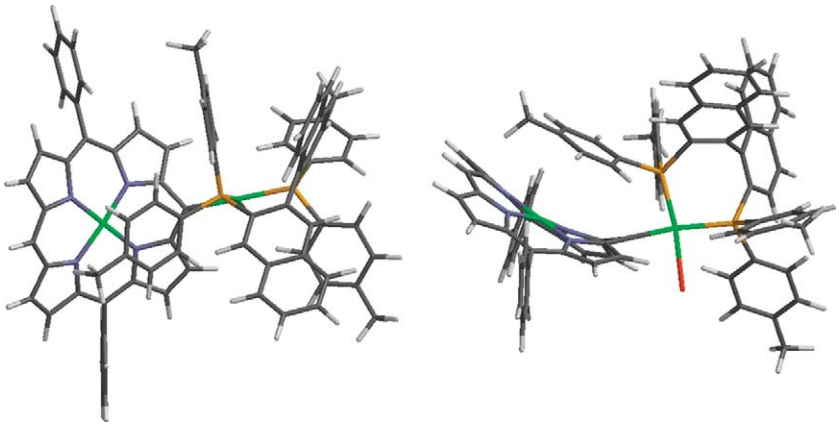

Fig. 3. The PM3 calculated equilibrium geometry for {PdBr(NiDPP)[(*R*)-Tol-BINAP]} (**3a**); left: top view; right: side view.

cooling to 258 K, this region reveals several signals, and indeed at 218 K (Fig. 2, lower), features at 5.30 and 5.64 ppm become notably sharper, with identical shapes to the 4.67/4.84 ppm pair discussed above. Simultaneously, the latter signals have broadened and shifted slightly upfield. In a mixture of $CD_2Cl_2/CDCl_3$ at 193 K, this region appears as one broad signal, suggesting that, at even lower temperatures, the two sides of this ring would be observed to be non-equivalent. The 5.30/5.64 signals integrate for only one H each. These results can be explained by rotation of the tolyl groups being slowed such that the two sides of the rings are detectably non-equivalent. The higher field set has a much lower coalescence temperature, due in part to a much smaller chemical shift difference between the pairs on each side of the ring. By examination of the model in Fig. 3, it seems that the highest field set represents the ring that lies across and nearly parallel to the porphyrin, while the set that is very broad at room temperature may be from the protons of the ring that is close to the porphyrin but nearly orthogonal to it. Other effects of the lowering of the temperature are seen in the downfield region, in the emergence of two sharp doublets at 8.35 and 8.58 ppm, whose presence was unsuspected on viewing the room temperature spectrum. From their typical chemical shifts, these are *o*-Hs of one of the 10,20-Ph rings. Overall, the combination of these experiments has given a picture of the complex that is fairly well matched to the calculated structure, although we would have liked to obtain a crystal structure to define some of these aspects somewhat more clearly. Unfortunately, efforts to grow single crystals were unproductive so far, as only powders were obtained, and long storage in solution led to decomposition.

The diphos complexes **4** exhibited similar asymmetry in the downfield region, and because of the relative simplicity and rigidity of the ligand, the 1D spectrum is much less complex. In common with the other complexes, the phenyl group on the P *cis* to DPP appears well upfield, the *ortho* protons resonating at 5.48 ppm. As noted above, it is unlikely that the complexes of this ligand could be used for any applications that depend on long-term storage, due to their instability in solution. However, catalytic asymmetric reactions may still be possible if the active species survive long enough for reactions such as transmetallations to occur.

2.3. UV–Vis and CD spectra

A major point of interest with these complexes, and indeed any porphyrins made asymmetric by appending chiral fragments, is how does the porphyrin chromophore react to the asymmetric environment. In Figs. 4–6, the UV–Vis and CD spectra of **2b**, **3a**,**b**, and **4a** are shown (optical spectra of **4a** were recorded immediately after preparation of the solutions to reduce the effect of unavoidable decomposition).

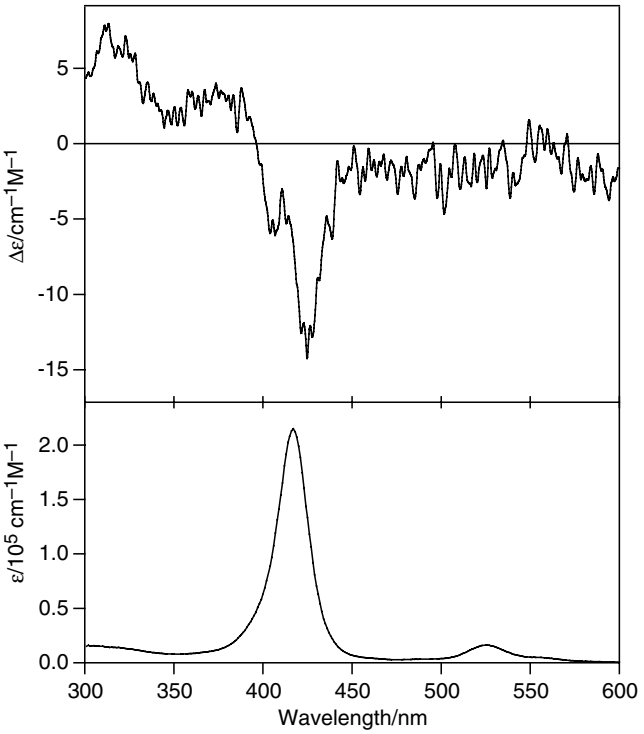

Fig. 4. CD spectrum (upper) and visible absorption spectrum (lower) of {PdBr(NiDPP)[(*R*,*R*)-diphos]} **4a** in CH_2Cl_2.

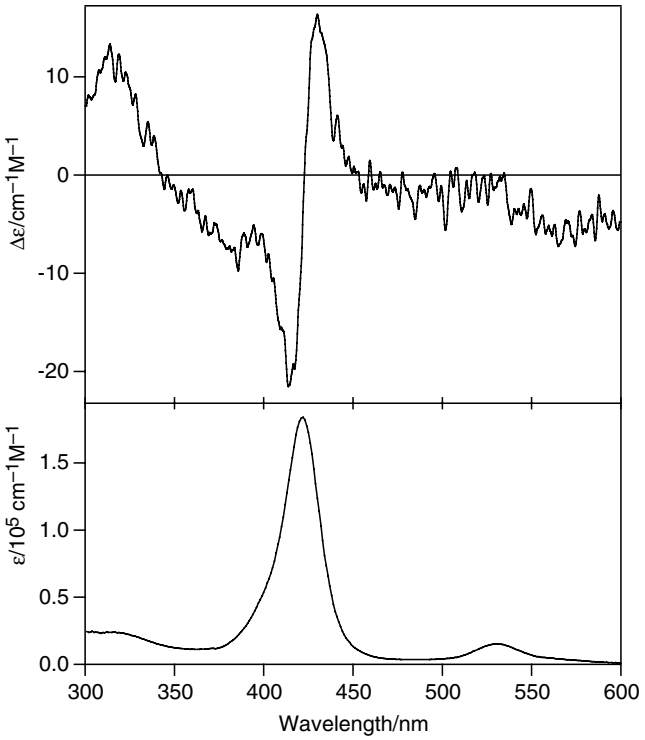

Fig. 5. CD (upper) and visible absorption (lower) spectra of {PdBr(NiDPP)[(*S*,*S*)-CHIRAPHOS]} **2b** in CH_2Cl_2.

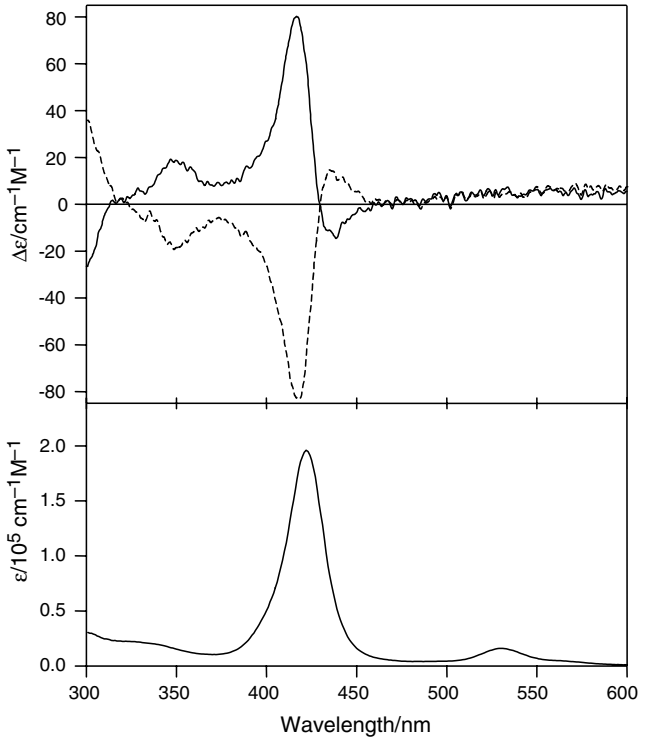

Fig. 6. CD spectrum of {PdBr(NiDPP)[(*R*)-Tol-BINAP]} (**3a**) (upper, solid line), {PdBr(NiDPP)[(*S*)-Tol-BINAP]} (**3b**) (upper, dashed line), and visible absorption spectrum (lower) in CH_2Cl_2.

The UV–Vis spectra of **2**–**4** show similar spectral patterns in the region of 300–600 nm, which are entirely typical of Ni(II) porphyrin complexes, characterized by an intense Soret band (corresponding to the allowed porphyrin B transition) and visible bands of low intensities (corresponding to the quasi-allowed porphyrin Q transitions) (Figs. 4–6, lower). It is of note that while the absorption maxima of **2** and **3** are exactly the same, the maxima of **4** are hypsochromically shifted by 5–7 nm. These high-energy shifts are apparently a result of smaller degree of the porphyrin ring distortion due to the less bulky diphos substituent in **4**.

On the basis of CD analysis (Figs. 4–6, upper), these complexes exhibit different efficiency of asymmetry transfer from a chiral substituent to the porphyrin core. Thus, in contrast to similar UV–Vis absorption properties, their chiroptical properties are rather dissimilar, reflecting their structural and conformational peculiarities. In general, CD in monomeric porphyrins can be induced by the chiral deformations of the porphyrin ring and/or by the through-space excitonic interactions between the porphyrin electronic transition and a different type of electronic transition (such as carbonyl or aromatic electric dipole moments), which are spatially fixed in a close proximity to the porphyrin ring in a chiral fashion. In the former case, the optical response is typically a monosignate CD signal reflecting inherent optical activity of the porphyrin electronic transitions [31,32], whilst the latter results in a bisignate couplet, often of unsymmetrical shape, if several excitonic couplings are involved [33,34]. For example, an appreciable coupled-oscillator interaction between the porphyrin π–π* transitions and π–π* transitions of aromatic groups was demonstrated in the case of heme containing proteins [35]. However, the CD outcome may be even more complicated, if both asymmetry transfer mechanisms operate simultaneously. In the chiral complexes studied, we may also expect existence of these two channels of chirality transfer because of considerable ruffling of the porphyrin core as clearly seen in Fig. 3 and the possibility of multiple excitonic interactions between the porphyrin and aromatic electronic transitions.

Hence, in the case of less crowded **4a**, the CD spectrum consists of two moderate negative Cotton effects (CE) at 425 and 413 nm ($\Delta\varepsilon = -14$ and -5 cm^{-1} M^{-1}, respectively) corresponding to the porphyrin B transitions (Fig. 4). This monosignate spectral pattern is apparently due to the inherent chiral deformations caused by the diphos substituent, whilst excitonic interactions of the porphyrin B transitions with phenyl electronic transitions apparently are rather weak or just cancelled each other due to a particular spatial arrangement. The situation is drastically changed upon increasing the substituent's bulkiness in **2b**. Surprisingly, a well defined and nearly symmetrical bisignate signal is clearly observed in the CD spectrum (Fig. 5). This couplet consists of two CEs of opposite signs with positive and negative CEs at 430 ($\Delta\varepsilon = +16$ cm^{-1} M^{-1}) and 414 ($\Delta\varepsilon = -21$ cm^{-1} M^{-1}) nm, respectively. The CE positions are bathochromically shifted in comparison to those of **4a**, following the corresponding UV–Vis patterns, and their

intensities are markedly enhanced; the zero crossing point is at 422 nm that matches exactly with the UV–Vis absorption maximum of the Soret band. These CD features are typical for exciton coupling and apparently arise from the through-space interactions between the porphyrin and phenyl electronic transitions. Judging from the positive sign of the induced CD, the (*S*,*S*)-CHIRAPHOS substituent and porphyrin chromophore couple with each other in an overall clockwise orientation [36].

Further increasing of the substituent bulkiness by introducing a binaphthyl group in **3a**,**b** results in even more profound effects in the CD spectra. In particular, the induced CD signal is of complex bisignate shape (Fig. 6) and consists of two non equivalent CEs in the region of Soret transitions at 436 and 418 nm, of different intensities ($\Delta\varepsilon = \pm 15$ and ± 80 cm^{-1} M^{-1}, respectively). The overall optical activities of **3a** and **3b** are further enhanced in comparison to those of **2b** and **4a**, while the zero crossing point is bathochromically shifted from the maximum of Soret band by 7 nm due to asymmetry of the induced couplet. These CD features are a result of the increased rotational strength of the coupling electronic transitions and multicomponent interchromophoric through-space interactions caused by the additional binaphthyl group. The sign of the CD couplet is directly dependent upon the substituent's absolute configuration with the (*R*)-enantiomer **3a** giving a negative first CE and (*S*)-enantiomer **3b** inducing CE of opposite sign, thus yielding the corresponding mirror images. According to the exciton chirality method [36], the sign of the induced chirality reflects the corresponding clockwise and anticlockwise orientations of the substituent–porphyrin interactions for **3b** and **3a**, although their complexity makes it difficult to assign the individual couplings.

3. Conclusion

We have demonstrated the original aim, i.e. the generation of a chiral porphyrin environment using single enantiomers of chelating diphosphine ligands on peripherally metallated organopalladium porphyrins. The Tol-BINAP ligand offers the most promise for further study, as it induces the strongest effects on the CD spectra, as well as forming fairly stable products. Clearly, for any application where coordination at the central metal ion of the metalloporphyrin is required, Ni(II) is not the ideal metal ion to choose. However, we have found in the past that Ni porphyrins give the cleanest NMR behaviour, hence their use in these preliminary studies. In future, we would like to extend this work into: (i) other centrally coordinated metals such as Zn(II), Mg(II) (for chiral recognition); (ii) five- or six-coordinate metals such as Co(III), Mn(III), Ru(II) (for enantioselective catalysis using the central metal); and (iii) less labile transition metals on the periphery, especially Pt, Rh, or Ir (to afford more stable compounds).

4. Experimental

4.1. General

Syntheses involving zerovalent metal precursors were carried out in an atmosphere of high-purity argon using conventional Schlenk techniques. The organopalladium porphyrins were handled in air once isolated. Reagents and ligands were used as received from Sigma–Aldrich, unless stated below. 5-Bromo-10,20-diphenylporphyrin and its nickel complex were prepared according to known procedures [37]. The enantiomerically pure chiral diphos ligands were supplied by Dr. S.B. Wild, Research School of Chemistry, The Australian National University, and the Tol-BINAP ligands (Strem) were supplied by Dr. M.L. Williams, School of Science, Griffith University. All solvents were of analytical reagent grade. Toluene and diethyl ether were stored over sodium wire. Dichloromethane and chloroform were stored over anhydrous sodium carbonate. THF was distilled immediately before use from sodium/benzophenone under an atmosphere of high-purity argon. Analytical TLC was performed using Merck silica gel 60 F_{254} plates and column chromatography was performed using Merck silica gel (230–400 mesh). ^{1}H NMR spectra were recorded on a Bruker Avance 400 MHz spectrometer and ^{31}P spectra were recorded on a Varian Unity 300 MHz instrument in $CDCl_3$ solutions, using $CHCl_3$ as the internal reference at 7.26 ppm for ^{1}H spectra, and external 85% H_3PO_4 as the zero reference for proton-decoupled ^{31}P spectra. The low temperature and 2D NMR studies were performed at the Centre for Molecular Architecture, Central Queensland University, on a Bruker Avance 400 MHz instrument. In Australia, UV–Vis spectra were recorded on a Varian Cary 3 spectrometer using dichloromethane as solvent. FAB mass spectra were recorded by the Mass Spectrometry Service, Research School of Chemistry, The Australian National University, using *m*-nitrobenzyl alcohol as matrix. Microanalyses were performed by the Microanalytical Service, Department of Chemistry, The University of Queensland. UV–Vis and CD spectra were measured in Japan at room temperature in CH_2Cl_2 solutions on a Shimadzu UV-3101PC spectrometer and JASCO J-720 spectropolarimeter, respectively. CD scanning conditions were as follows: scanning rate = 50 nm/min, bandwidth = 2 nm, response time = 1 s, accumulations = 4.

4.2. Synthesis of {PdBr(NiDPP)[(R,R)-CHIRAPHOS]} (**2a**)

Toluene (5 ml) was added to a Schlenk flask and heated to 105 °C under a stream of Ar. (*R*,*R*)-CHIRAPHOS (17.0 mg, 0.0399 mmol) was added, followed by Tris-(dibenzylideneacetone)-dipalladium(0) (Pd_2dba_3, 18.3 mg, 0.0199 mmol). The dark purple colour of the palladium starting material faded, leaving a clear dark yellow solution. After stirring for a further 5 min, Br(NiDPP)

(11.9 mg, 0.0199 mmol) was added, and the mixture was stirred at 105 °C for 2 h, and the reaction progress was monitored by TLC (CH_2Cl_2:hexane, 1:1). After cooling to room temperature, the volume was reduced to about one-third under vacuum, and hexane was added to precipitate the product, which was filtered, washed with hexane and vacuum dried to yield a fine dark purple powder (17.1 mg, 76%). ^{1}H NMR: δ 0.80 (dd, J(P–H) 12.8, J(H–H) 6.8 Hz, 3H, CH_3 nearer to P *cis* to DPP), 1.03 (dd, J(P–H) 10.2, J(H–H) 6.8 Hz, 3H, CH_3 nearer to P *trans* to DPP), 2.13 (m, J(P–H) 11.3 Hz, 1H, CH nearer to P *trans* to DPP), 2.65 (m, J(P–H) 11.1 Hz, 1H, CH nearer to P *cis* to DPP), 5.24 (m, 4H, *o*- and *m*-H of one PPh), 5.56 (qt, 1H, *p*-H of one PPh), 7.07 (dt, 2H, *m*-H of one PPh), 7.23 (dt, 1H, *p*-H of one PPh), 7.40 (br dd, 2H, *o*-H of one PPh), 7.5–7.72 (m, 16H, PPh and 10,20–Ph), 8.08–8.2 (overlapping m, 4H, *o*-H of two PPh), 8.29, 8.45 (each d, 1H, $J = 4.7$ Hz, 2- and 8-β H), 8.73, 8.75 (each d, 1H, $J = 4.7$ Hz, 12- and 18-β H), 8.89, 8.99 (each d, 1H, $J = 4.7$ Hz, 13- and 17-β H), 9.27, 9.41 (each d, 1H, $J = 4.7$ Hz, 3- and 7-β H), 9.57 (s, 1H, *meso*-H) ppm. ^{31}P NMR: δ 41.8 (d, J_{PP} 38.5 Hz), 58.9 (d, J_{PP} 38.5 Hz).

4.3. Synthesis of {PdBr(NiDPP)[(S,S)-CHIRAPHOS]} (**2b**)

This complex was prepared by the method above for **2a** using 10 ml of toluene, (*S*,*S*)-CHIRAPHOS (12.8 mg, 0.0300 mmol), Pd_2dba_3 (13.7 mg, 0.0150 mmol) and Br(NiDPP) (11.9 mg, 0.0199 mmol) to yield a fine purple powder (22.2 mg, 99%). NMR spectra were identical to those of the above enantiomer. UV–Vis: λ_{max} (ε/10^3 M^{-1} cm^{-1}) 422 (184), 530 (14.9), 560 sh (4.4) nm. FAB-MS (most abundant mass): 1131.18 (MH^+ calcd. 1131.09). Found: C, 63.76; H, 4.23; N, 4.49. $C_{60}H_{47}BrN_4NiP_2Pd$ requires C, 63.72; H, 4.19; N, 4.95%.

4.4. Synthesis of {PdBr(NiDPP)[(R)-Tol-BINAP]} (**3a**)

Toluene (10 ml) was added to a Schlenk flask and heated to 105 °C under a stream of Ar. (*R*)-Tol-BINAP (54.3 mg, 0.0800 mmol) was added, followed by Pd_2dba_3 (18.0 mg, 0.0197 mmol). The dark purple colour of the palladium starting material lightened to a dark orange solution. After stirring for a further 10 min, Br(NiDPP) (11.9 mg, 0.0199 mmol) was added. The reaction mixture was maintained at 105 °C under Ar for 5 h and monitored by TLC (ethyl acetate:hexane, 3:7). The mixture was cooled to room temperature and the solvent removed under high vacuum. The product **3a** was recrystallised from CH_2Cl_2–hexane in 80% yield as a fine dark purple powder. ^{1}H NMR (293 K): δ 0.31, 1.70, 2.06 and 2.53 (each s, 3H, CH_3), 4.67 (dd, 2H, Ptol), 4.84 (dd, 2H, Ptol), 5–6.5 (vbr, Ptol), 6.60 (m, 4H, Ptol), 6.9–7.8 (m, Naph, Ptol and 10,20-Ph), 7.9–8.1 (m, Ptol), 8.31 (t, 1H, Ptol), 8.3–8.6 (vbr, Ptol), 8.59, 8.71, 8.76, 8.80, 8.96, 8.98, 9.81, 10.02 (each 1H, d, β-H), 9.58 (1H, s, *meso*-H) ppm. ^{31}P NMR: δ 11.9 (d, J_{PP} 37.4 Hz), 25.0 (d, J_{PP} 37.4 Hz). UV–Vis: λ_{max} (ε/10^3 M^{-1} cm^{-1}) 422 (196), 530 (15.8), 560 sh (4.8) nm. FAB-MS: weak cluster peaking at 1382.3 (M^+ calcd. 1382.2).

4.5. Synthesis of {PdBr(NiDPP)[(S)-Tol-BINAP]} (**3b**)

This complex was prepared by the method above using (*S*)-Tol-BINAP. The enantiomers exhibited identical NMR and UV–Vis spectra, as expected.

4.6. Synthesis of {PdBr(NiDPP)[(R,R)-diphos]} (**4a**)

Toluene (6 ml) was added to a Schlenk flask and heated to 105 °C under a stream of Ar. (*R*,*R*)-diphos (19.4 mg, 0.0602 mmol) was added, followed by Pd_2dba_3 (27.5 mg, 0.0300 mmol). The dark purple colour of the palladium starting material lightened to a dark orange solution. After stirring for a further 10 min, Br(NiDPP) (11.9 mg, 0.0199 mmol) was added. The reaction mixture was maintained at 105 °C under Ar and monitored by TLC (CH_2Cl_2-hexane, 3:7). After 15 min, a dark precipitate was noted. After 30 min, the reaction mixture was cooled and the precipitate was collected by vacuum filtration and dried under high vacuum to yield **4a** (57%) as a dark purple powder. ^{1}H NMR: δ 1.02 (d, J(P–H) 10.6 Hz, 3H, CH_3), 2.59 (d, J(P–H) 9.1 Hz, 3H, CH_3), 5.51 (dd, 2H, *o*-H on PPh *cis* to DPP), 6.01 (dt, 2H, *m*-H on PPh *cis* to DPP), 6.69 (br t, 1H, *p*-H on PPh *cis* to DPP), 7.4–7.7 (series of m, 15H, PPh, ligand Ph and *m*-, *p*-H of 10,20-Ph), 7.8–7.9 (m, 4H, *o*-H of 10,20-Ph), 8.14, 8.73, 8.76, 8.77, 8.85, 9.06, 9.07, and 9.41 (each d, 1H, β-H), 9.72 (s, 1H, *meso*-H) ppm. ^{31}P NMR: δ 44.2 (d, J_{PP} 23.3 Hz), 36.3 (d, J_{PP} 23.3 Hz). UV–Vis: λ_{max} (ε/10^3 M^{-1} cm^{-1}) 417 (215), 525 (17), 553 sh (5.1) nm. FAB-MS: 1026.2 (M^+ calcd. 1024.02).

4.7. Synthesis of {PdBr(NiDPP)[(S,S)-diphos]} (**4b**)

This complex was prepared by the method above using (*S*,*S*)-diphos. The enantiomers exhibited identical NMR spectra. These complexes were both unstable in $CDCl_3$ solution, with significant decomposition to form NiDPP evident within 1 h.

Acknowledgements

We thank Dr. S.B. Wild and Dr. M.L. Williams for gifts of chiral ligands. M.J.H. thanks the Faculty of Science, Queensland University of Technology, for a Post-graduate Scholarship. We thank Dr. M.R. Johnston and the Centre for Molecular Architecture, Central Queensland University for the use of their NMR facilities for parts of the work.

References

[1] K.M. Kadish, K.M. Smith, R. Guilard (Eds.), The Porphyrin Handbook, vol. 1–10, Academic Press, San Diego, 2000.

[2] H. Ogoshi, T. Mizutani, Accounts Chem. Res. 31 (1998) 81.
[3] J.-C. Marchon, R. Ramasseul, in: K.M. Kadish, K.M. Smith, R. Guilard (Eds.), The Porphyrin Handbook, vol. 11, Elsevier Science, San Diego, 2003, p. 75.
[4] M. Claeys-Bruno, M. Bardet, J.-C. Marchon, Magn. Reson. Chem. 40 (2002) 647.
[5] J.-P. Simonato, J. Pécaut, J.-C. Marchon, Inorg. Chim. Acta 315 (2001) 240.
[6] J.-P. Simonato, S. Chappellet, J. Pécaut, P. Baret, J.-C. Marchon, New J. Chem. 25 (2001) 714.
[7] C.Z. Wang, Z.A. Zhu, Y. Li, Y.T. Chen, X. Wen, F.M. Miao, W.L. Chan, A.S.C. Chan, New J. Chem. 25 (2001) 801.
[8] R. Schwenninger, J. Schlögl, J. Maynollo, K. Gruber, P. Ochsenheim, H.-B. Bürgi, R. Konrat, B. Kräutler, Chem. Eur. J. 7 (2001) 2676.
[9] P. Le Maux, M. Lukas, G. Simonneaux, J. Mol. Catal. A 206 (2003) 95.
[10] C.-M. Che, J.-S. Huang, F.-W. Lee, Y. Li, T.-S. Lai, H.-L. Kwong, P.-F. Teng, W.-S. Lee, W.-C. Lo, S.-M. Peng, Z.-Y. Zhou, J. Am. Chem. Soc. 123 (2001) 4119.
[11] G. Reginato, L. Di Bari, P. Salvadori, R. Guilard, Eur. J. Inorg. Chem. (2000) 1165.
[12] V.V. Borovkov, G.A. Hembury, Y. Inoue, Accounts Chem. Res. 37 (2004) 449.
[13] X. Huang, B.H. Rickman, B. Borhan, N. Berova, K. Nakanishi, J. Am. Chem. Soc. 120 (1998) 6185.
[14] A. Sugasaki, K. Sugiyasu, M. Ikeda, M. Takeuchi, S. Shinkai, J. Am. Chem. Soc. 123 (2001) 10239.
[15] H. Tsukube, N. Tameshige, S. Shinoda, S. Unno, H. Tamiaki, Chem. Commun. (2002) 2574.
[16] Y. Mizuno, T. Aida, Chem. Commun. (2003) 20.
[17] A. Sugasaki, M. Ikeda, M. Takeuchi, A. Robertson, S. Shinkai, J . Chem. Soc., Perkin Trans. 1 (1999) 3259.
[18] Y. Kubo, T. Ohno, J.-i. Yamanaka, S. Tokita, T. Iida, Y. Ishimaru, J. Am. Chem. Soc. 123 (2001) 12700.
[19] (a) For some examples combining palladium and chiral diphosphines in catalysis, see: D. Bruyere, N. Monteiro, D. Bouyssi, G. Balme, J. Organomet. Chem. 687 (2003) 466;
(b) A.B. Dounay, K. Hatanaka, J.J. Kodanko, M. Oestreich, L.E. Overman, L.A. Pfeifer, M.M. Weiss, J. Am. Chem. Soc. 125 (2003) 6261;
(c) C. Larksarp, O. Sellier, H. Alper, J. Org. Chem. 66 (2001) 3502;
(d) O. Hamed, P.M. Henry, Organometallics 17 (1998) 5184;
(e) H. Brunner, K. Kramler, Synthesis (1991) 1121.
[20] P.J. Brothers, Adv. Organomet. Chem. 46 (2001) 223, and references therein.
[21] D.P. Arnold, Y. Sakata, K.-i. Sugiura, E.I. Worthington, Chem. Commun. (1998) 2331.
[22] D.P. Arnold, P.C. Healy, M.J. Hodgson, M.L. Williams, J. Organomet. Chem. 607 (2000) 41.
[23] M.J. Hodgson, P.C. Healy, M.L. Williams, D.P. Arnold, J. Chem. Soc., Dalton Trans. (2002) 4497.
[24] R.D. Hartnell, A.J. Edwards, D.P. Arnold, J. Porphyr. Phthalocya. 6 (2002) 695.
[25] R.D. Hartnell, D.P. Arnold, Eur. J. Inorg. Chem. (2004) 1262.
[26] R.D. Hartnell, D.P. Arnold, Organometallics 23 (2004) 391.
[27] A. Kato, R.D. Hartnell, M. Yamashita, H. Miyasaka, K.-i. Sugiura, D.P. Arnold, J. Porphyr. Phthalocya. 8 (2004) 1222.
[28] F. Atefi, O.B. Locos, D.P. Arnold, unpublished results.
[29] Y. Chen, G.-Y. Gao, X.P. Zhang, Tetrahedron Lett. 46 (2005) 4965.
[30] (a) A.M. McDonagh, M. Cifuentes, M.G. Humphrey, S. Houbrechts, J. Maes, A. Persoons, M. Samoc, B. Luther-Davies, J. Organomet. Chem. 610 (2000) 71;
(b) M.J. McKeage, P. Papathanasiou, G. Salem, A. Sjaarda, G.F. Swiegers, P. Waring, S.B. Wild, Metal-Based Drugs 5 (1998) 217;
(c) A. Bader, T. Nullmeyers, M. Pabel, G. Salem, A.C. Willis, S.B. Wild, Inorg. Chem. 34 (1995) 393.
[31] K. Konishi, T. Sugino, T. Aida, S. Inoue, J. Am. Chem. Soc. 113 (1991) 6487.
[32] K. Konishi, K. Miyazaki, T. Aida, S. Inoue, J. Am. Chem. Soc. 112 (1990) 5639.
[33] T. Mizutani, T. Ema, T. Yoshida, Y. Kuroda, H. Ogoshi, Inorg. Chem. 32 (1993) 2072.
[34] D. Liu, D.A. Williamson, M.L. Kennedy, T.D. Williams, M.M. Morton, D.R. Benson, J. Am. Chem. Soc. 121 (1999) 11798.
[35] M.-C. Hsu, R.W. Woody, J. Am. Chem. Soc. 93 (1971) 3515.
[36] N. Harada, K. Nakanishi, Circular dichroic spectroscopyExciton Coupling in Organic Stereochemistry, University Science Books, Mill Valley, CA, 1983.
[37] D.P. Arnold, R.C. Bott, H. Eldridge, F. Elms, G. Smith, M. Zojaji, Aust. J. Chem. 50 (1997) 495.